Nomenclature

LATIN SYMBOLS			GREEK SYMBOLS		
Symbol	Description	Unit	Symbol	Description	Unit
CL	Lift coefficient	——	ε	Camber ratio	——
Cd	Drag coefficient	——	σ	Maximum thickness ratio	——
P	Local pressure	Pa			
P_∞	Atmospheric pressure	Pa	ρ	Fluid density	kg/ m^3
C_p	Pressure coefficient	——	α	Two dimensional geometric angle of attack	degree
Re	Reynolds Number	dimensionless			
T	Thickness distribution	m	θ	Camber line slope	degree
Cc	Chord Wise force coefficient	——	**Abbreviations**		
Δx	Distance step in x-direction	m	Symbol	**Description**	
Δy	Distance step in y-direction	m	NACA	**National Advisory Committee of Aeronautics**	
N	Normal force	N			
c	Airfoil Chord	m	NASA	**National Aeronautics and Space Administration**	
L	Lift force	N			
D	Drag force	N			
A	Axial force	N			
U	Fluid velocity	N/m			
N	Local unit outward normal vector	——			
F	Force	N			
CS	Control surface	——			
V	Velocity	m/s			

Introduction

The control of boundary layer is the significance of aircraft engineering design of wing. The lift and drag coefficients vary markedly during different condition of flight. Low drag coefficients are partially emphasized in modern wing designs to increase the range of flight. The accurate predictions of flow developments around airfoil configurations remain a difficult phenomena in the field around such airfoil. The regions of separation is the important one in boundary layer of flow around airfoil and are common in many engineering applications. Separation is the entire process in which the boundary layer flow breaks down and departs from the wall surface. Most of flow fields with separation will have a region of flow where the 'law-of-the-wall' holds.

(Simpson1991) has observed that the mean flow upstream of incipient detachment obeys the law-of-the-wall and law-of-the-wake if the following conditions is met: the maximum shear stress is less than 1.5 times the wall shear stress as (Th. Lutz 2003). In flight tested by NASA research center (Cook 1974),on cylinder located at the leading edge of the flaps are made to rotate at high speed with flaps in a lowered position. The test program was to assess handling qualities of the propeller powered STOL-type aircraft at higher lift coefficient. The aircraft flown at speed of 29-31m/s along approaches up to (-8°)which corresponded to a lift coefficient of about 4.3.

(Modi1988)carried out tests on rotating cylinders located at the leading and trailing edge of the airfoil. The leading edge rotating cylinder extends the lift curve without affecting its slope thus increasing the maximum lift and delaying stall. The trailing edge cylinder acts as a flap and shifts the lift curve to the left thus increasing the lift coefficient before stalling occur. There are many ways to control of boundary likes using sound to control boundary layer or using very small extended surfaces starting from body that want to control the boundary layer on(Y. Khalighi2008, Hsaiao1990, Mohammed W.K.2007). (Ahmed Z. Al-Garni2000) shows an experimental investigation conducted on a two-dimensional NACA 0024 airfoil equipped with a leading-edge rotating cylinder. The work showed that the leading-edge rotating cylinder increases the lift coefficient of a NACA 0024 airfoil from 0.85 to 1.63 when the cylinder surface velocity ratio increase from 0 to 4 and delays the stall angle of attack by about 160%.

(Zaman1987) produced the relation between lift coefficient and angle of attack degree as in **Fig.1**. (C. Y. Zhou2004) studied a circular cylinder in the trailing edge of NACA 4412 airfoil in a cross flow is numerically using finite volume method for Reynolds Number Re=200 based on the cylinder diameter The results indicate that the existence of an upstream airfoil has significant impacts on the drag and lift on the cylinder, the vortex pattern and the vortex shedding frequency, and also the presence of a circular cylinder in the near wake of the airfoil can cause flow to separate earlier and the separation point to move upwards. There is a rapid rise in drag coefficient on the

cylinder at L/D=3.5 for the case of to the case of α=15° which shows, to some extent, a similarity to the case of two tandem cylinders; force coefficients on the cylinder and shedding frequency increases with L/D. While (Salam H.H.2005) produced a good theoretical research for control boundary layer about airfoil NACA 0012. In this research try to experiment the effect of circular cylinder on the boundary layer behavior around the airfoil NACA 0012, when it location at the leading edge of this airfoil with angles of attack (0°,5°,10°,14° and 20°). The result of this experimental work will compared with his results.

Experimental Procedure

The measurements was done on the test section of a wind tunnel with air flow speed 24 m/s with airfoil NACA 0012 has dimensions shown in **Fig.2** and the subsonic wind tunnel shown in **Fig.3** and the airfoil NACA 0012 inside the wind tunnel without cylinder at the leading edge of the airfoil shown in **Fig.4**, then a circular cylinder composed at the leading edge of airfoil NACA 0012 with gap (1mm) shown in **Fig.5**, the dimensions of circular cylinder shown in **Fig.6**. First, the manometer calibrated with digital air flow manometer at different speeds and get a good convergence as in **Fig.7.** The manometer was used to measure the static pressure around airfoil NACA 0012 for angle of attack (0°,5°,10°,14° and 20°) on the upper and lower surfaces shown in **Fig.8**. The static pressure around airfoil NACA 0012 measured without circular cylinder at the leading edge of it and then circular cylinder was putting as shown in **Fig.4** and **Fig.5** respectively. At this time the static pressure will measured again around airfoil with same angles of attack. The drag and lift coefficient was calculated using the integration by Simpson rule for upper and lower surfaces of airfoil. The Smoke wind tunnel shown in **Fig.9** was used to visualization the stream lines behavior around airfoil without circular cylinder before the airfoil and with circular cylinder at the leading edge of the airfoil with the same angles of attack(0°, 5°, 10° , 14° and 20°) to investigate the circular cylinder effect on the boundary layer transpose around the airfoil and especially the separation regions.

Airfoil Geometry and Coordinate System

To analysis the aerodynamic characteristic of airfoils that used in this work must be known airfoil geometry. Most of the airfoils generation was based on simple shape definitions that emerged as a result of improved understanding of airfoil performance and the ability to design new airfoils using computer methods, the NACA airfoils are still useful in many aerodynamic design applications. Most of new references study the older NACA airfoils together with the new airfoils.

The NACA airfoils are constructed by combining a thickness envelope with a camber or mean line. The equations, which describe this procedure, are (Haider.K.R. 2009):

$$\begin{aligned} x_u &= x - y_t(x)\sin\theta \\ y_u &= y_c(x) + y_t(x)\cos\theta \end{aligned} \tag{1}$$

$$\begin{aligned} x_L &= x + y(x)\sin\theta \\ y_L &= y_c(x) - y_t(x)\cos\theta \end{aligned} \tag{2}$$

where $y_t(x)$ is the thickness function, $y_c(x)$ is the camber line function, and

$$\theta = \tan^{-1}\left(\frac{dy_c}{dx}\right) \tag{3}$$

It is unusual to neglect the camber lone slope, which simplifies the equations and makes the reverse problem of extracting the thickness envelope and mean line for given airfoil straightforward. The NACA four and five digit series are defined completely by formulas. In both cases, the thickness distribution is (Salam H.H.2005):

$$T(x) = \sigma c\left[1.4845\sqrt{\frac{x}{c}} - 0.6300\frac{x}{c} - 1.7580\left(\frac{x}{c}\right)^2 + 1.4215\left(\frac{x}{c}\right)^3 - 0.5075\left(\frac{x}{c}\right)^4\right] \tag{4}$$

The parameter σ is the thickness ratio of the airfoil (Maximum thickness/chord). This thickness distribution was derived in Eastman Jacob 1930, of the National advisory Committee for Aeronautics Langley Laboratory, on the basis of examination of airfoil's known to be efficient. The first digit of the 4 digit airfoil's destination is the maximum value of the mean line (camber ratio ε) in hundredths of chord, while the second digit is the chord wise position of the maximum chamber in tenths of the chord. The last two digit are the maximum thickness ratio, σ, in percent chord.

Aerodynamic Characteristics

(Schlichting 1968) shows the application of the momentum conservation laws that the forces and moments on an airfoil or a wing are due to two sources, (i) pressure distribution on the surface of the body, (ii) shear stress distribution over the surface of the body. The pressure forces act normal to the surface of the airfoil whereas the shear stress acts tangential to the surface of the

airfoil. The integration of these two distributions over the surface of the airfoil yields a resultant force and a moment. This resultant force can be divided into two components, one perpendicular. To the chord line, the normal force (N) and the other parallel to the chord line, the axial force (A) as (Raikan 2001). According to the law of conservation of momentum, the net rate of change of the momentum of the fluid crossing a control volume bounded by a control surface is equal to the sum of all external forces acting on the control volume. This is expressed as in (Haider K.R. 2009).

$$\sum F = \frac{\partial}{\partial t} \iiint_{CV} \rho u dv + \iint_{CS} \rho u (u.n) dS \qquad (5)$$

where (u) is the fluid velocity entering or leaving the control surface (CS) depending on whether (u.n) is negative or positive and (n) is a local unit outward normal vector to an element of area (dS) of the control surface. (∑F) is the resultant of all surface forces (pressure and shear) and all body forces (gravity).

Two Dimensional Wing Pressure Distribution

Whether determined from actual measurements or from potential flow theory, an integration can be performed to calculate the overall pressure force on the body. It is convenient to determine components of this force in the chord wise and normal direction. From **Fig.10** (Salam H.H.2005)get:

$L = N \cos \alpha - C \sin \alpha$

$D = N \sin \alpha + C \cos \alpha$

and yield in coefficient form

$CL = Cn \cos \alpha - Cc \sin \alpha \qquad (6)$

$Cd = Cn \sin \alpha + Cc \cos \alpha \qquad (7)$

At small angles of attack(α), the chord wise force coefficient, (Cc) is very small compared to the normal force coefficient, (Cn) and because (sin α) is much smaller than (cosα), the cumulative order of magnitude of the product (Cc sin α) is much smaller than (Cn cos α). Hence, we neglect the (Cc sinα) term and eq(6) reduces to

$$CL = Cn \cos\alpha \quad (8)$$

However, both terms on the right hand side of eq(8) are of the same order of magnitude and must be retained. Note that the drag coefficient, (Cd) in eq(7) is due only to surface pressure distribution and does not include the skin friction drag In order to determine the normal and chord wise force coefficients, we consider the effect of pressure on the upper and lower surfaces of elemental areas at the same chord-wise location on the airfoil and get the pressure coefficient (Cp) by eq(9). The Geometry of airfoil NACA0012 can be seen in **Fig.11** as (Jeppe Johansen1999).

$$Cp = \frac{P_{\infty} - P}{\frac{1}{2}\rho \mathrm{v}^2} \quad (9)$$

Results and Discussions

The relation between pressure distributions around airfoil NACA 0012 and pressure coefficient (Cp) as eq.(9) was calculated using Simpson rule, and by using eq.(7) the drag coefficient was calculated for each angle of attack. Also, the lift coefficient was compute in same way but using eq.(8). The drag coefficient and lift coefficient are very important parameter to check the separation point and boundary layer behaviors. **Fig.12** represent the relation between the angle of attack and lift coefficients of airfoil NACA 0012 with and without circular cylinder at the leading edge of it. For comparison the lift coefficient for other researcher shown in **Fig.1** with same Reynolds number Re= $1x10^5$. As shown in **Fig.12** the lift coefficient will increase as the angle of attack increase until the angle 15 degree that will be maximum they will reduce until angle of attack 20 degree . But, the lift coefficient will variants when there is a cylinder at the leading edge of it because the effect of cylinder appeared at low angle of attack since, the flow stream separate by cylinder before reach aerofoil until angle 10 degree, the stream will act on the airfoil and produce a pressure difference around this airfoil. The angle of attack 14 degree is the angle of separation for this airfoil without cylinder, if the cylinder putting at the leading edge of the airfoil, the separation at this angle will reduce; the reason is the separation point will be behind the airfoil. The lift coefficient still not stable because of vortex that generation at up surface of airfoil. The drag coefficient can be shown for the same system in **Fig.13**. As shown in this figure the drag will be very small at low angle of attack, but at higher than 10 degree increase as the angle of attack increase until the angle 15 degree that will be maximum then will reduce until angle of attack 20

degree and very irregular because of the cylinder effect. If the angle of attack increases more than 20degree, the drag force will increase too and become very high and the lift force will be not able to lift the air plane this mean the work will be useless. The irregularity will occur with turbulent flow produced by cylinder and applied on airfoil. The visualization of flow stream can be summarized experimentally using smoke wind tunnel as shown in **Fig.14** and **Fig.15**. It can be shown in these figures the behavior of boundary layer around airfoil with and without circular cylinder was perfectly shown, also it shows the turbulent flow will very clearly with cylinder but, at angle of attack 14 degree the separation occurs without cylinder. Also, with cylinder the separation point will change and turbulent intensity will increase. At 14 degree there are vortex generation and no separation of boundary layer. The separation of boundary layer occur when at angle of attack 20 degree when cylinder put at the leading edge of the airfoil.

Conclusions

1.There are differences between the values of the lift and drag coefficients without using circular cylinder and with circular cylinder arrange at the leading edge of the airfoil NACA 0012. The values of the lift and drag coefficients will variation in very irregular when there is a circular cylinder at the leading edge of airfoil . The lift coefficient will increase as the angle of attack increase until the angle 15 degree that will be maximum they will reduce until angle of attack 20 degree. The flow stream separate by cylinder before reach aerofoil until angle 10 degree, the stream will act on the airfoil and produce a pressure difference around this airfoil.

2.The angle of attack 14 degree is the angle of separation for this airfoil without cylinder at the leading edge of the airfoil, but the separation at this angle will not appears as the circular cylinder putting at the leading edge of the airfoil, the vortex will generated at this angle as the cylinder will change the angle of attack so the separation point will be behind the airfoil.

3. The drag coefficient will be very small at low angle of attack but at higher than 10 degree increase as the angle of attack increase until the angle 15 degree that will be maximum then will reduce until angle of attack 20 degree and very irregular. The irregularity will occur with turbulent flow produced by cylinder and applied on airfoil.

4.The angle of attack 20 degree is the angle of separation of the boundary layer if the circular cylinder compose at the leading edge of the airfoil as the flow stream separated by cylinder before reach aerofoil.

References

Ahmed Z. Al-Garni, Abdullah M. Al-Garni, Saad A. Ahmed, and Ahmet Z. Sahin" Flow Control for an Airfoil with Leading-Edge Rotation: An Experimental Study", Journal of Aircraft, Vol.37,No.4 http://eprints.kfupm.edu.sa/9330/1/Flow_Control_Airf_JAircraft_p1.pdf,August 2000

C. Y. Zhou, C. W. Sun, Y. Zhou, and L. Huang," A Numerical Study Of A Circular Cylinder In The Wake Of An Airfoil",15 Australasian Fluid Mechanics Conference, http://www.aeromech.usyd.edu.au/15afmc/proceedings/papers/AFMC00204.pdf ,December 2004.

Haider K.R. " Study of Flow Induced Noise in Rectangular Test Sections with an Obstruction " Thesis, PhD. University of Technology ,2009

Hsaiao, F.B.,Liu, C.F.,and Shyu, J.Y.," Control of Wall Separated Flow by Internal Acoustic Excitation", AIAA Hournal,Vol.28,No.8,p.1440-1446,1990.

Jeppe Johansen "Unsteady Airfoil Flows with Application to Aeroelastic Stability", http://130.226.56.153/rispubl/VEA/veapdf/ris-r-1116.pdf, October1999.

Modi,V.J. and Mokhtarian, F.,"Effect of Moving Surfaces on the Airfoil Boundary Layer Control", Aircraft J., Vol.27,No.1,pp.42-50,1988.

Mohammed W. K. " The Effect of the Internal Acoustic Excitation on the Aerodynamic Characteristics of Airfoil" Thesis, University of Technology, 2007.

Raikan S.D., "Proposal for Subsonic Wind Tunnel Suitable in Iraq" Thesis, M.Sc., University of Baghdad, September 2001.

Salam H. H.," Incompressible Flow over An Airfoil with Rotating Cylinder" Thesis, PhD. University of Baghdad, 2005.

Simpson,R.L.," The Structure of the Near-wall Region of Two Dimensional Turbulent Separated Flow ,"Phil. Trans. RSoc.Lond.A,Vol336,pp.5-17,1991

Schlichting, H., " Boundary Layer Theory ", McGraw-Hill, 6th edition, 1968.

Th. Lutz, W. Wurz, A. Herrig, K. Braun, and S. Wagner "Numerical Optimization of Silent Airfoil Sections" Institut für Aerodynamik und Gasdynamik (IAG), Universitat Stuttgart, Pfaffenwaldring 21, D-70550 Stuttgart, 2003.

Y. Khalighi, A. Mani, F. Ham and P. Moin." Prediction of sound generated by complex flows at low Mach number regimes", Center for Turbulence Research Annual Research Briefs, p.p313-324, http://ctr.stanford.edu/ResBriefs08/23_khalighi.pdf ,2008.

Zaman,K.B., BAR-Sever, and Mangalam,S.M.. "Effect of Acoustic Excitation on the Flow over low-Re Airfoil", J. Fluid Mech.Vol. 182 pp.127-148,1987.

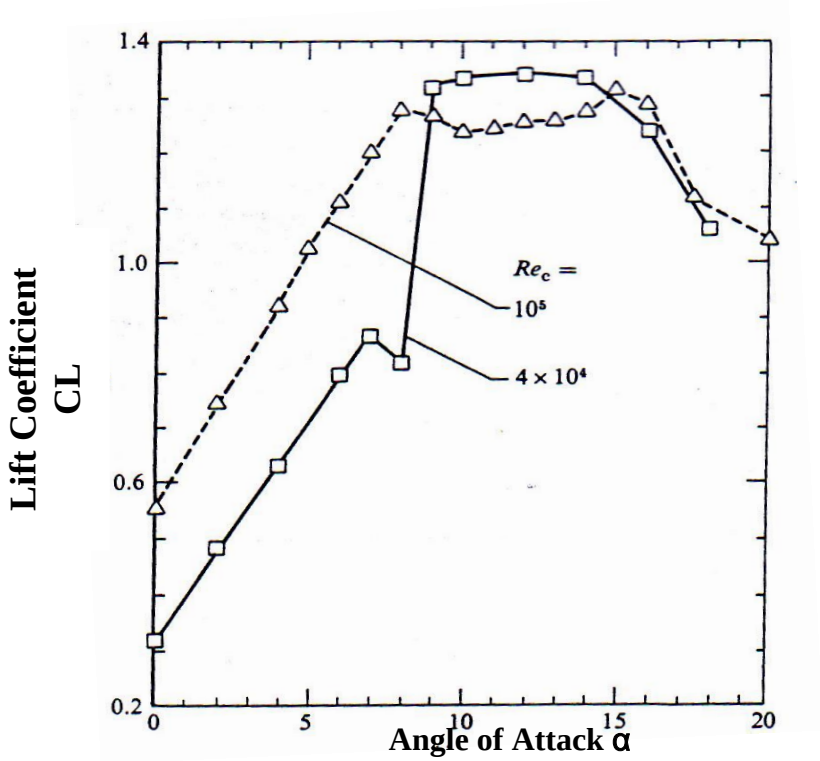

Fig.1 Relation between Lift Coefficient and Angle of Attack Degree

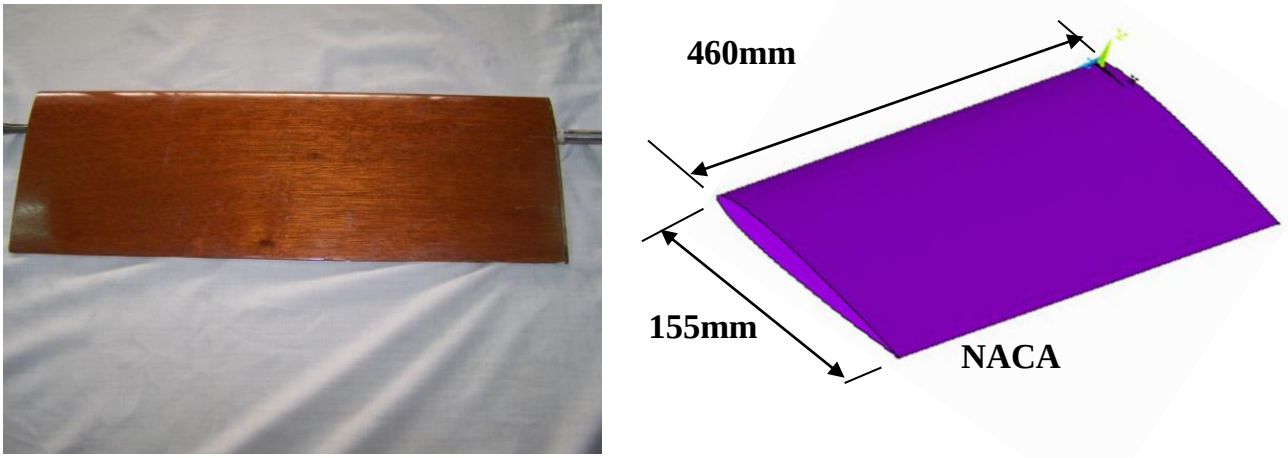

Fig.2 Airfoil NACA 0012 Dimensions

Fig.3 Subsonic Wind Tunnel.

Fig.4 Airfoil NACA 0012 inside Wind Tunnel without Circular Cylinder.

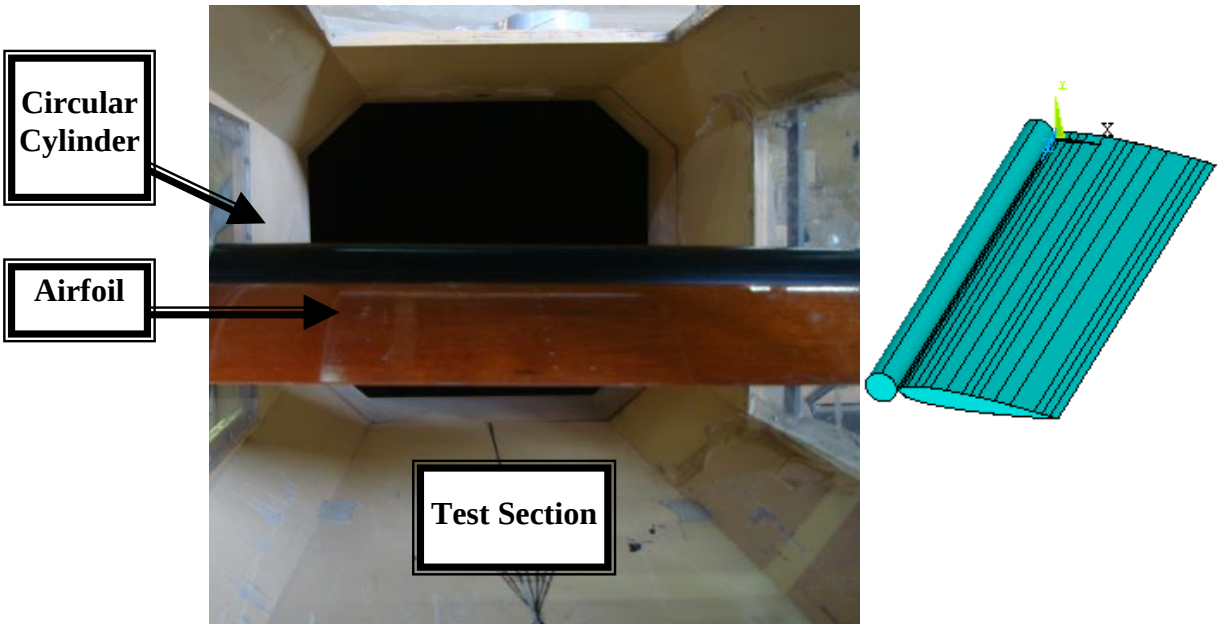

Fig.5 Airfoil NACA 0012 inside Wind Tunnel with Circular Cylinder (Gap 1mm).

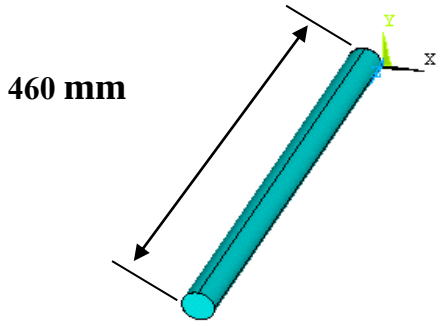

Fig.6 Circular Cylinder with D= 30mm

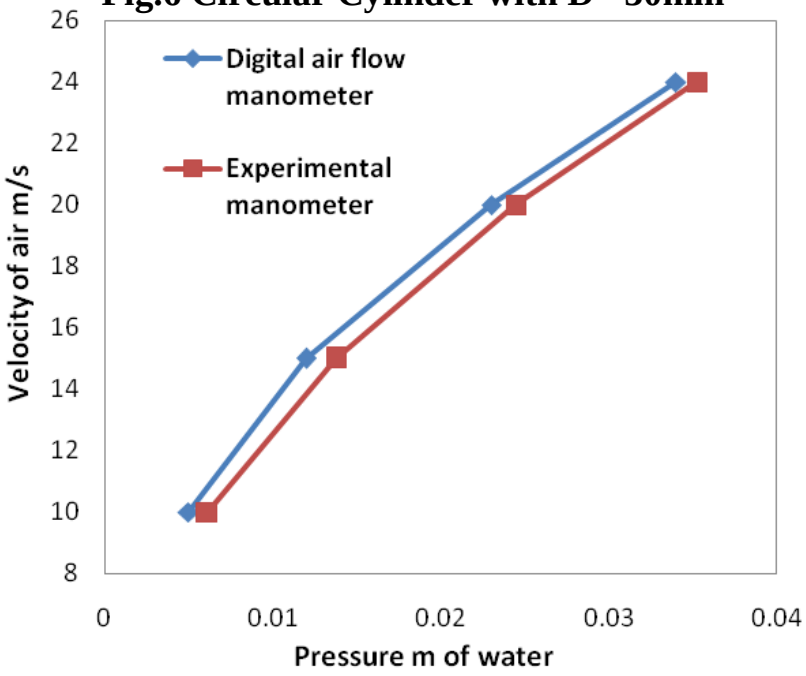

Fig.7 Velocity-Pressure Calibration Curve

Fig.8 Manometer used to Measure the Static Pressure around Airfoil

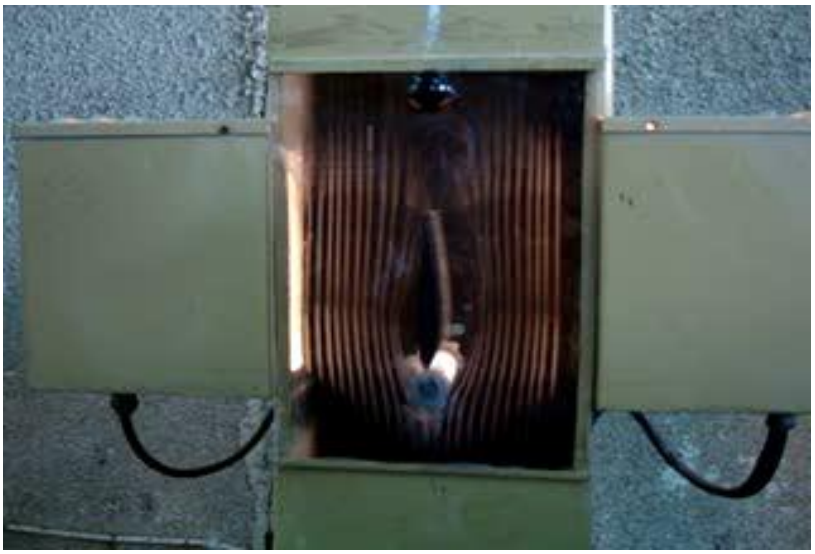

Fig.9 Smoke Wind Tunnel

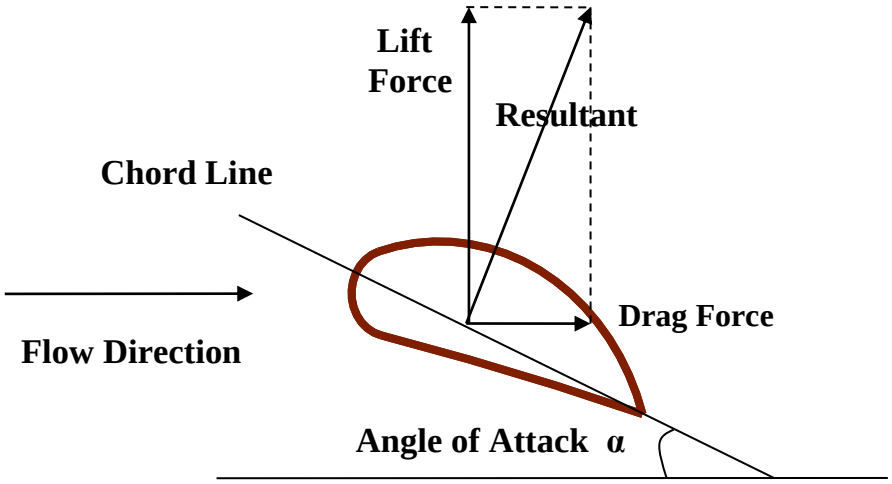

Fig.10 Lift and Drag Force Act by Flow over Airfoil

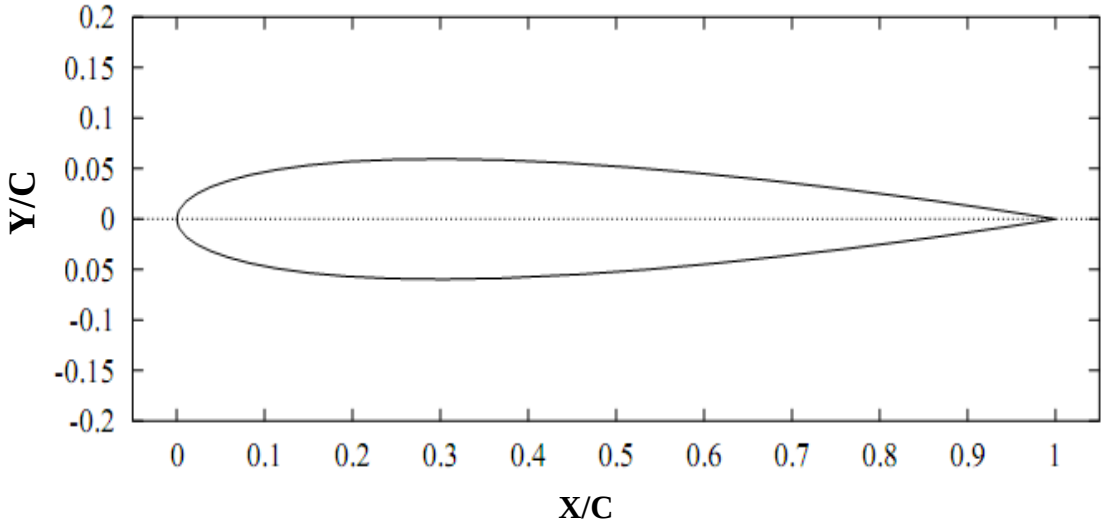

Fig.11 Airfoil NACA 0012

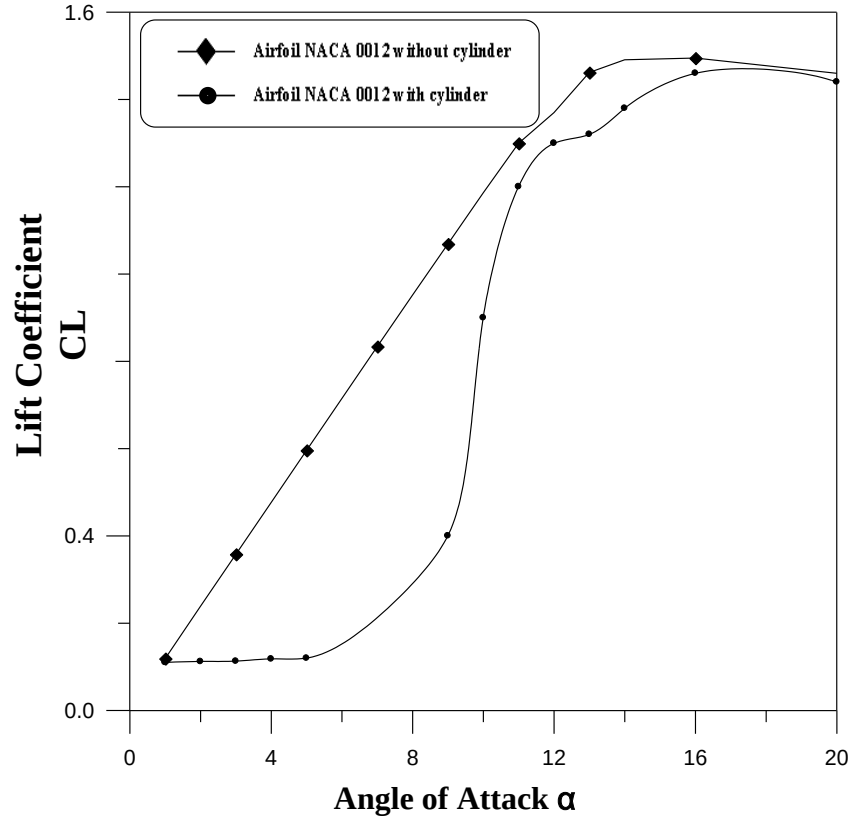

Fig.12 Relation between Lift Coefficient and Angle of Attack Degree

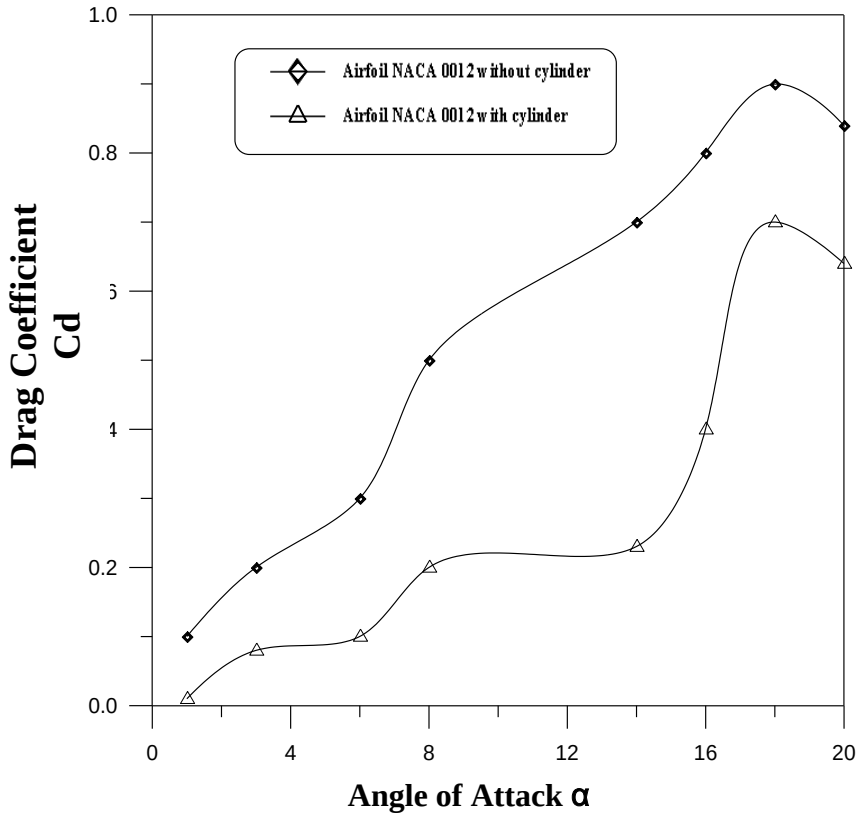

Fig.13 Relation Between Drag Coefficient and Angle of Attack Degree.

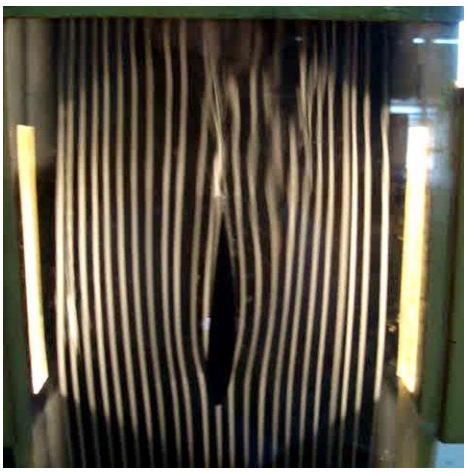

Angle of attack= 0°

Angle of attack= 5°

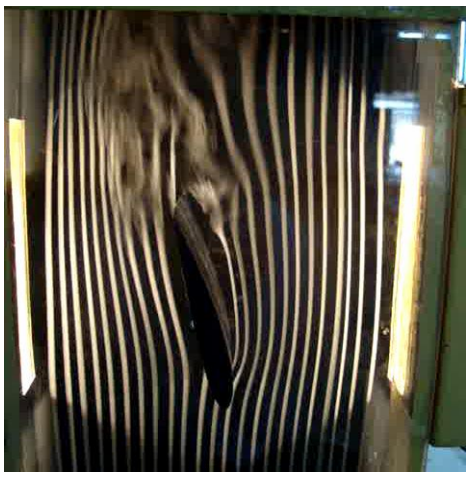

Angle of attack=10°

Angle of attack=14°

Angle of attack=20°

Fig.14 Flow Visualization of Flow at Angles of Attack 0°, 5°,10°,14° and 20° Respectively Around Airfoil Without Cylinder.

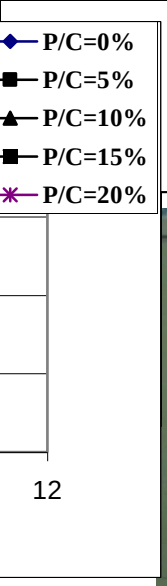

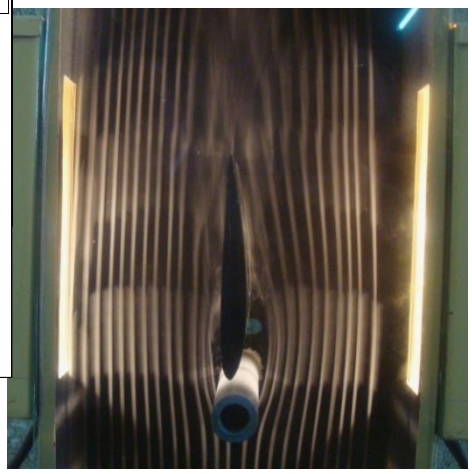

Angle of attack= 0°

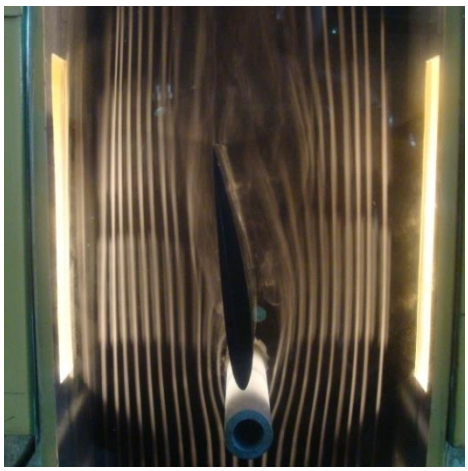

Angle of attack= 5°

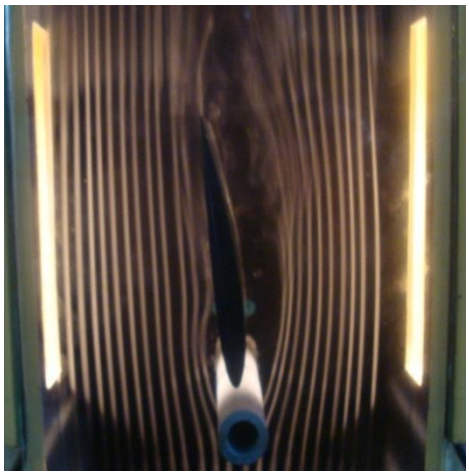

Angle of attack=10°

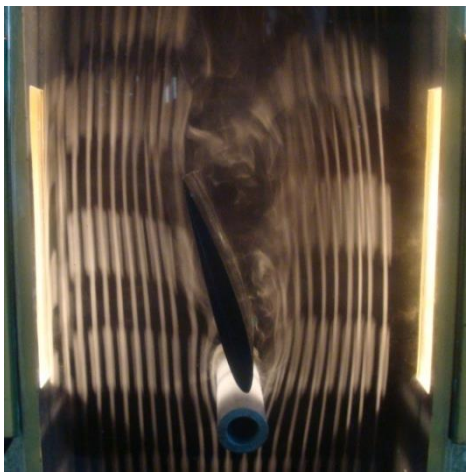

Angle of attack=14°

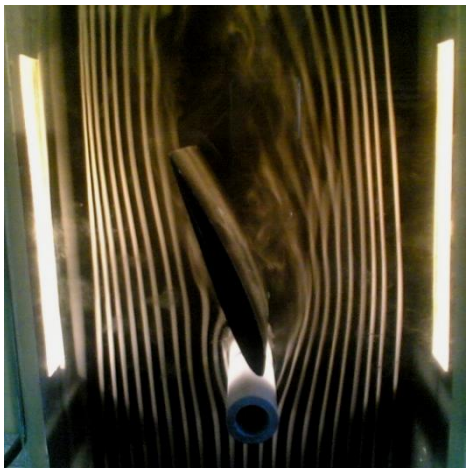

Angle of attack=20°

Fig.15 Flow Visualization of Flow at Angles of Attack 0°, 5°,10°,14° and 20° Respectively Around Airfoil With Cylinder.